Green Chemistry

Accepted Manuscript

This is an *Accepted Manuscript*, which has been through the RSC Publishing peer review process and has been accepted for publication.

Accepted Manuscripts are published online shortly after acceptance, which is prior to technical editing, formatting and proof reading. This free service from RSC Publishing allows authors to make their results available to the community, in citable form, before publication of the edited article. This *Accepted Manuscript* will be replaced by the edited and formatted *Advance Article* as soon as this is available.

To cite this manuscript please use its permanent Digital Object Identifier (DOI®), which is identical for all formats of publication.

More information about *Accepted Manuscripts* can be found in the **Information for Authors**.

Please note that technical editing may introduce minor changes to the text and/or graphics contained in the manuscript submitted by the author(s) which may alter content, and that the standard **Terms & Conditions** and the **ethical guidelines** that apply to the journal are still applicable. In no event shall the RSC be held responsible for any errors or omissions in these *Accepted Manuscript* manuscripts or any consequences arising from the use of any information contained in them.

View Online

Cite this: DOI: 10.1039/c0xx00000x

www.rsc.org/xxxxxx

ARTICLE TYPE

Ce promoted Pd-Nb catalysts for γ-valerolactone ring-opening and hydrogenation

R. Buitrago[a], J.C. Serrano-Ruiz[a], F. Rodríguez-Reinoso[a], A. Sepúlveda-Escribano[a]*, J.A.Dumesic[b]

Received (in XXX, XXX) Xth XXXXXXXXX 20XX, Accepted Xth XXXXXXXXX 20XX

DOI: 10.1039/b000000x

γ-valerolactone (GVL) has been catalytically transformed into pentanoic acid (PA), a molecule of growing importance in the search of alternative green fuels and chemical feedstocks. The GVL conversion process goes through ring-opening and hydrogenation reactions over well dispersed Pd-NbCe oxides on an activated carbon support.

1. Introduction

The search for new energy sources that allow the reduction of the extensive use of fossil fuels is nowadays one of the main research fields. In this sense, the conversion of biomass-derived compounds to liquid hydrocarbon fuels similar to those obtained from oil is a potential alternative, as the use of these green hydrocarbons does not require special changes in the current distribution infrastructure and in the engine mechanism[1].

In general, there are three significant biomass sources that can be used to produce biofuels: starchy feedstocks (sugars included), triglyceride feedstocks and lignocellulosic material[2]. In fact, lignocellulose alone offers an energy supply larger than the current rate of consumption[3]. The production of liquid hydrocarbon fuels from lignocellulosic derivatives requires the removal of oxygen functionalities and the formation of C-C bonds, with the control of the molecular weight of the final hydrocarbons and the use of lesser amounts of hydrogen from external sources[4].

γ-valerolactone (GVL) has been identified as an important chemical platform that can be obtained from lignocellulosic biomass and, through different processes, it can be transformed into liquid hydrocarbon fuels for the transportation sector. One of the most promising routes to upgrade GVL involves the intermediate production of valeric acid (pentanoic acid, PA) by means of ring opening and subsequent hydrogenation on a bifunctional metal/acid catalyst[5,6].

Niobium-based materials and, especially, niobium oxide, have been shown to be useful in a wide range of catalytic processes such as pollution abatement, selective oxidation, hydrocarbon conversion reactions, hydrogenation and dehydrogenation, hydrotreating, carbon monoxide hydrogenation, dehydration and hydration, photocatalysis and electrocatalysis, and polymerization. This behaviour is a consequence of its redox and surface acidity properties [7,8]. With regard to the transformation of GVL into PA, the acidity of niobia is useful for the ring-opening reaction to yield pentenoic acid. In a second state, pentenoic acid has to be hydrogenated to PA and, to this end, an active metal such as Pd is needed. In this way, Serrano-Ruiz et al.[5] have shown that a Pd-Nb catalyst has good performance in the ring-opening/hydrogenation tandem reactions.

On the other hand, ceria is a partially reducible oxide whose surface reducibility is strongly enhanced in the presence of a noble metal, which not only lowers the reduction temperature but also increases the extent of reduction. Furthermore, partial reduction treatments at relatively high temperature (about 773 K) of ceria-supported metals induce the so-called Strong Metal-Support Interaction (SMSI) effect, by which the catalytic behaviour of the metal is strongly modified. The interaction between the ceria support and the active metal depends on the extent of the interface region, which is increased when using high surface area ceria. It has been shown that small ceria crystallites can be obtained by dispersing this oxide on the surface of a high surface area support such as carbon, and that this approach can be used to enhance the catalytic behaviour in different reactions[9-12]. With this in mind, this study reports the beneficial effect of homogeneously dispersing a Nb-Ce mixed oxide on a carbon support, so that small particles are obtained, thus enhancing the catalytic behaviour of Pd in the GVL ring opening/hydrogenation as compared to regular materials such as Pd-Nb. The obtained results are explained on the basis of enhanced redox properties and acidity of the final catalyst.

2. Experimental

2.1 Catalyst Preparation

The bulk oxides, pure Nb_2O_5 and Nb_2O_5 doped with 10 wt.% CeO_2 (NbCe), were prepared by homogeneous precipitation with urea, whereas the carbon supported oxides were prepared by wet impregnation of the carbon support with the minimum amount of aqueous solutions containing ammonium niobate(V) oxalate hydrate ($NH_4[NbO(C_2O_4)_2(H_2O)]\cdot(H_2O)_m$, Sigma Aldrich, 99.99%) and hydrated cerium nitrate $Ce(NO_3)_3\cdot6H_2O$ (Sigma-Aldrich, 99.99%) as precursors. 1 wt.% palladium was subsequently added by wet impregnation with aqueous solutions, using palladium nitrate dihydrate (Sigma-Aldrich ~40 wt.% Pd basis) as the metal precursor. The carbon support was an industrial activated carbon, RGC-30 (from MeadWestvaco, Charleston. NC, USA) prepared by phosphoric acid activation.

The carbon was ground and meshed (200 - 300 μm), and stored in the oven at 373 K overnight before impregnation with aqueous solutions of the oxide precursors. Dried carbon was added to the solution (10 mL per gram of support) under stirring. After 12 h in a rotary evaporator, the solvent was slowly removed by vacuum. Finally, the solid was heat treated during 5 h at 623 K under flowing helium (50 mL min^{-1}), with a heating rate of 1 K min^{-1}, in order to slowly decompose the metal precursors, trying to avoid the modification of the carbon surface by the nitrogen oxides evolved from nitrate decomposition[12]. In this way, activated carbon was loaded with a 20 wt.% of Nb_2O_5 and NbCe oxides (Nb-C and NbCe-C). Finally, 1 wt.% of Pd was loaded by wet impregnation with aqueous solutions of palladium nitrate. All samples were treated in a He flow 50 mL/min 5 hours at 623 K. The samples are labelled as Pd-Nb, Pd-NbCe for the pure and modified oxide supports, and Pd-Nb-C, Pd-NbCe-C for the carbon-supported oxides.

2.2 Catalyst Characterization

The textural properties of the prepared materials were determined by nitrogen adsorption at 77 K on a Coulter Omnisorp 610 system. The samples were dried at 383 K for 12 h and out-gassed at 523 K under vacuum before performing the analysis. The micropore volume, V_{micro}, was obtained by application of the Dubinin–Radushkevich (DR) equation to the adsorption isotherms. The mesopore volume, V_{meso}, was estimated by subtracting the micropore volume from the uptake at a relative pressure of 0.95. The surface area was calculated by application of the BET method.

X-ray powder diffraction patterns were recorded on a JSO Debye-flex 2002 system, from Seifert, fitted with a Cu cathode and a Ni filter, using a 2° min^{-1} scanning rate.

RAMAN spectroscopy analysis was carried out on a LabRam spectrometer (Jobin-Yvon Horiba). The excitation source was a He-Ne laser (632 nm) with a power of 50 mW. The beam was focalized using a 50x lens. The monochromator used is a 600 slit cm^{-1}. The detector was a CCD (1064 x 256 pixels), and the acquisitions were taken by 15 seconds with 3 accumulations.

Temperature-programmed reduction (TPR) measurements were carried out in a U-shaped quartz cell using a 5% H_2/He gas flow of 25 cm^3 min^{-1} and about 0.15 g of sample, with a heating rate of 10 K min^{-1}. Hydrogen consumption was followed by on-line mass spectrometry.

Conventional TEM analysis was carried out with a JEOL model JEM-210 electron microscope working at 200 kV and equipped with a INCA Energy TEM 100 analytical system and a GATAN model ORIUS SC600 camera. Samples for analysis were suspended in methanol and placed on copper grids with a holey-carbon film support.

Temperature-programmed desorption (TPD) of NH_3 was used to measure the number of acid sites on the catalysts. Samples were placed in a quartz tubular reactor placed in a furnace with thermal control. The effluent was monitored by a mass spectrometer Pfeiffer (OminStar 301). Before the TPD experiments, the samples were cleaned with in a helium flow of 50 mL min^{-1} at 573 K for 2 hours. Then, the sample was cooled to 298 K and put in contact with a NH_3 (99.99% purity) flow of 70 mL min^{-1} during 20 min. Then, the physisorbed NH_3 was removed by flowing helium at 373 K until a stable signal was obtained. Desorption of strongly adsorbed NH_3 was performed by heating the catalyst at a rate of 10 K min^{-1} under flowing helium (50 mL min^{-1}), from room temperature to 1173 K.

X-Ray photoelectron spectra (XPS) were acquired with a VG-Microtech Multilab 3000 spectrometer equipped with a hemispherical electron analyzer and a Mg Kα (h = 1253.6 eV, 1 eV = 1.6302 x 10^{-19} J) 300 W achromatic X-ray source. Previous to the XPS measurements, samples were submitted to an ex-situ reduction treatment at 538 K for 3 h with flowing H_2 (100 mL min^{-1}) and a heating rate of 5 K min^{-1}, similar to that used before the catalytic tests. Reduced samples were placed in micro-centrifuge tubes containing n-octane, under flowing helium to avoid contact with air. Finally, several drops of the n-octane slurry containing the sample were placed in a sample rod and introduced in the pre-treatment chamber, where the solvent was removed with flowing N_2. Finally, the sample was moved to the analysis chamber, where it was maintained until a residual pressure of ca. 5 x 10^{-7} N m^{-2} was reached. The spectra were collected at a pass energy of 50 eV, and measurements were taken using a take-off angle of 45°. Survey scans were taken in the range 0-1100 eV and high resolution scans were obtained on all significant peaks in the survey spectra. The intensities were estimated by calculating the integral of each peak, after subtraction of the S-shaped background, and by fitting the experimental curve to a combination of Lorentzian (30%) and Gaussian (70%) lines. All binding energies (B.E.) were referenced to the C 1s line at 284.6 eV, which provided binding energy values with an accuracy of ± 0.2 eV.

2.3 Catalytic Studies

The catalytic studies were carried out in a ¼´´ tubular stainless steel reactor at 598 K and 34 bar controlled by a back-pressure regulator. The catalyst (0.5g) was loaded between two end-plugs of quartz wool (Grace) before being tested, and reduced at 538 K for 3 h with flowing hydrogen (100 mL min^{-1}, 5 K min^{-1}). Then it was heated to 598 K at 1 K min^{-1} in a hydrogen flow of 50 mL min^{-1}. Once the catalyst reached the target temperature, a He 20 mL min^{-1}-H_2 80 mL min^{-1} flow and an aqueous solution of GVL (60 wt.%) were fed into the reactor containing the catalyst. CO and CO2 with a Shimadzu GC-8A (equipped with TCD detector and an Alltech packed column model HayeSep DB 100/120) and gaseous alkanes with a Varian GC (Saturn 3) using a FID detector and a GS-Q capillary column (J&W Scientific). The liquid phase products were drained from the separator and analysed by GC (Shimadzu GC-2010, FID, SHRX5 column) and by GC-MS (Shimadzu GC-2010 SHRX1-5MS column).

3. Results and Discussion

3.1 Catalysts characterization

Table 1 shows the BET surface area (N_2, 77K), the micropore volume (V_{micro}, N_2, 77 K, DR) and the volume of mesopores (V_{meso}) for the parent carbon and for the different supports (bulk oxides and carbon-supported oxides).

The N_2 adsorption isotherms for all the carbon based materials (Supplementary information) corresponded to Type I isotherms,

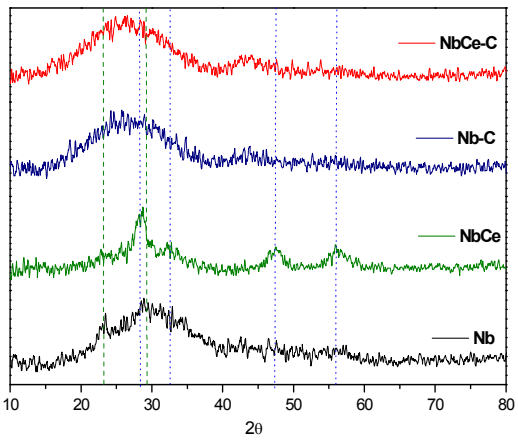

Fig 1. X-ray diffraction patterns of the supports.

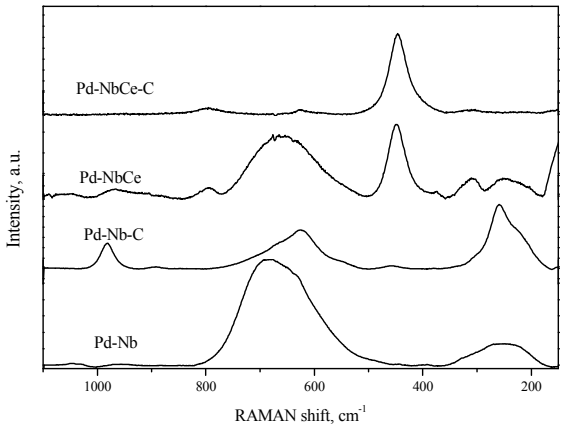

Fig 2. RAMAN spectra of the catalysts.

which are characteristic of microporous materials. However, there is also a given amount of mesoporosity, as the adsorption and desorption branches were not coincident (hysteresis loop) above a relative pressure of 0.5. The S_{BET} of the parent support decreased as a result the presence of the Nb and the Nb-Ce oxides. On the other hand, the bulk oxides showed a much lower BET surface area as compared to carbon-supported materials. It is interesting to note that the addition of ceria strongly decreased the surface area of pure Nb_2O_5, although the herein obtained values are comparable to those reported in the literature for similar materials. Thus, Védrine et al.[13] prepared niobic oxide with a surface area ranging from 140 to 35 $m^2 g^{-1}$ by hydrolysis of $NbCl_3$ in aqueous solution with ammonia and calcination at different temperatures(e.g. from 383 to 773 K). Similarly, Ouchi et al.[14] prepared niobic oxide with different hydration degrees by calcination of niobic acid at different temperatures (473 to 1073 K). They found a strong effect of the calcination temperature on the surface area of niobic oxide, which ranged from 125 $m^2 g^{-1}$ (calcination at 473 K) to 3 $m^2 g^{-1}$ (calcination at 1073 K). Remarkably, after calcination at 673 K they obtained a material with a surface area of 95 $m^2 g^{-1}$, which is noticeably lower than that of our Nb sample calcined at 623 K (199 $m^2 g^{-1}$, Table 1).

Table 1. Textural properties of supports.

	S_{BET} ($m^2 g^{-1}$)	V_{micro} ($cm^3 g^{-1}$)	V_{meso} ($cm^3 g^{-1}$)
C	1487	0.54	0.62
NbCe	81	0.04	0.03
NbCe-C	1066	0.45	0.40
Nb	199	0.05	0.07
Nb-C	1102	0.46	0.40

The XRD spectra of the supports (Fig. 1) showed broad bands due to the relatively amorphous character of these materials and their small crystallite size. The diffraction bands were even broader for the carbon-supported oxides, this being indicative of a high dispersion of the oxides on the carbon support. The dashed lines show the position of the main diffraction bands for the hexagonal TT-Nb_2O_5 phase (JCPDS [07-0061]). Weak signals at these positions were only obtained for the bulk oxides. The dotted lines indicate the position of the diffraction peaks corresponding to the fluorite-type structure of cerium oxide (JPDS [34-0394])[15]. Again, they were evident only for the bulk cerium-doped niobia material (NbCe).

Taking into account the calcination temperature used in the preparation of the oxides, the most likely structure obtained is the hexagonal TT-Nb_2O_5 phase and, effectively, a brief inspection of the RAMAN spectra of the catalysts shown in Fig. 2 evidenced the typical bands reported for this structure. Thus, a broad asymmetric and intense band centred at 690 cm^{-1} is assigned to vibrations (symmetric and anti-symmetric stretching mode) of Nb-O-Nb bridges with nearly octahedral niobia oxide species; the bands at 200-300 cm^{-1} are characteristics of the bending modes of Nb-O-Nb linkages and, finally, the bands at 900 – 990 cm^{-1} are characteristics of the symmetric stretching mode of the Nb=O terminal double bond[16-19].

An intense peak centred at 460 cm^{-1} can be seen in the spectra corresponding to the cerium-containing catalysts, which is assigned to the symmetric stretching mode of the Ce-O with F_{2g} symmetry[20,21].

It is interesting to note that the Raman bands corresponding to niobium species in the carbon-supported catalysts are much less intense than those for the catalysts supported on the bulk oxides. This could be due to the lesser amount of oxide in the supported samples, but this is discarded as the signal for CeO_2 at 460 cm^{-1} is similar for the carbon-supported and the carbon-free samples. One tentative explanation is that carbon-supported niobia species are more amorphous, and this would be in agreement with XRD results. On the other hand, the Raman spectra obtained for catalyst Pd-Nb-C show a well-defined band near 1000 cm^{-1}, which is assigned to Nb=O species in highly-distorted NbO_6 octahedra[19]. Thus, it can be concluded that the dispersion of the oxides on the carbon support strongly modifies the structural properties of the niobia species.

Fig. 3 presents the TEM images of the carbon-supported niobia and ceria-doped niobia samples. The micrographs corroborate the information given by XRD and N_2 adsorption. In particular, a high dispersion of the oxides on the carbon support was achieved, with no large particles or aggregates being formed. Furthermore,

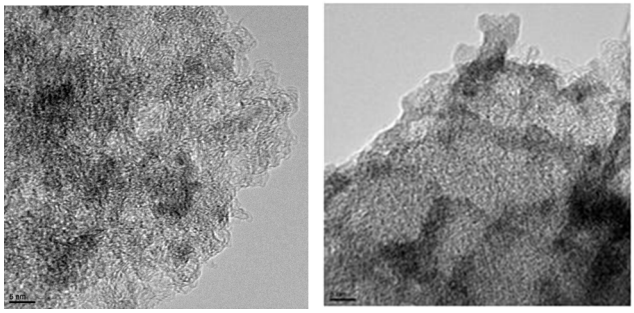

Fig 3.TEM micrographs of the Nb-C(left) and NbCe-C(right) support (scale bar 5 nm).

the surface morphology of the catalysts seems not to be modified with the addition of cerium oxide.

The characterization of the acidic properties of the different catalysts was carried out by NH_3-TPD. Fig. 4 shows the NH_3 desorption profiles obtained. The profiles for the parent C support were included for the sake of comparison. The typical NH_3-TPD profile of niobic acid calcined at 623 K shows a broad band centred at about 573 K[22]. Calcination at higher temperatures decreases the acidity, yielding a lower amount of ammonia adsorbed[23]. Except for the parent carbon support, a broad band of ammonia desorption, assigned to adsorption on the niobia surface, was observed for all materials. Significant differences were found in the NH_3 profiles of the catalysts supported on bulk oxides and those containing carbon-supported materials. Thus, the amount of ammonia adsorbed on the carbon-supported catalysts was much higher, thus indicating a larger amount of acidic sites in these materials. This difference can be explained in terms of a higher dispersion of the oxide on the activated carbon, which favours the formation of smaller particles with larger exposed surfaces. The TPD profiles of Pd-Nb-C and Pd-NbCe-C catalysts showed two overlapped desorption bands with maxima at slightly different temperatures, thus indicating the presence of surface sites with different acid strength in similar proportion. In conclusion, the dispersion of the oxide promoters on the carbon surface highly enhanced the amount of acid surface sites, which, as will be detailed below, play an important role in the GVL to PA conversion process.

Fig. 5 shows the Ce 3d XP spectra obtained with both Ce-containing catalysts after reduction at 528 K. The complexity of these spectra, with was first resolved by Burroughs et al.[24], arises from the hybridization between Ce 4f levels and the O 2p states. The two sets of spin-orbital multiplets, corresponding to the $3d_{3/2}$ and $3d_{5/2}$ contributions, are labelled with u and v, respectively, and up to four peaks for each contribution can be obtained by deconvolution, as shown in Fig. 5[25-27]. The peaks labelled v and v'' are ascribed to a mixing of Ce $3d^9$ $4f^2$ O $2p^4$ and Ce $3d^9$ $4f^1$ O $2p^5$ Ce(IV) final states, and the peak denoted v''' corresponds to the Ce $3d^9$ $4f^0$ O $2p^6$ Ce(IV) final state. On the other hand, lines v_0 and v' are assigned to the Ce $3d^9$ $4f^2$ O $2p^5$ and the Ce $3d^9$ $4f^1$ O $2p^6$ of Ce(III). The same assignation can be applied to the u structures, which correspond to the Ce $3d_{3/2}$ levels. The deconvolution of these experimental spectra allows calculation of the degree of ceria reduction[28], which can be obtained from the ratio between the sum of the intensities of the u_0, u', v_0 and v' bands and the sum of the intensities of all the bands:

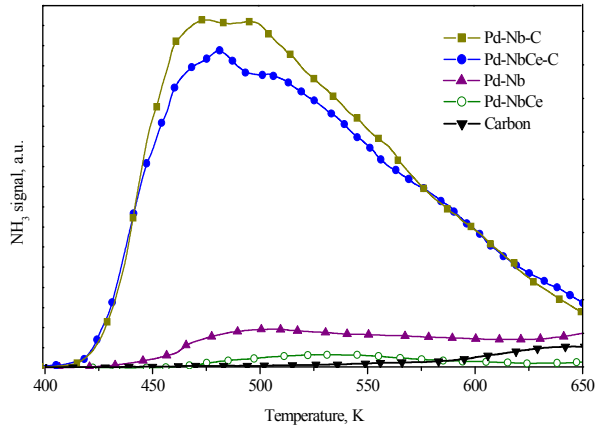

Fig 4. NH_3-TPD profiles of the catalysts

$$Ce(III) = 100 \times [S(u_0)+S(u')+S(v_0)+S(v')] / \sum[S(u)+S(v)]$$

Thus, the percentages of reduction of Ce for Pd-NbCe and Pd-NbCe-C after the reduction treatment at 538 K were, respectively, 46.9 and 64.9 %. It has been shown that Ce(IV) ions can be partially reduced during XPS experiments[26]. One of the parameters that affects the photoreduction of CeO_2 during XPS analysis is its crystallinity, in such a way that amorphous cerium oxide samples are reduced more extensively than crystalline materials[29]. Thus, these XPS results indicate that ceria is much more reducible when dispersed on the carbon support, more likely because of a smaller particle size and lower crystallinity when deposited on the carbonaceous material. This higher reducibility could affect the catalytic behaviour of palladium through a strong interaction effect by which partially reduced ceria, an "n" type semiconductor, would modify the electronic properties of the metal[30].

The Nb 3d XP spectra for the samples reduced at 538 K are shown in Fig. 6. They are composed of a doublet corresponding to the $3d_{3/2}$ and $3d_{5/2}$ levels. These bands are tabulated to be centered at 210.1 and 207.3 eV, respectively, for Nb_2O_5[31,32]. It can be seen from Fig. 6 that, for the catalysts reported in this study, only the bands obtained with the Ce-containing samples were centered at those values (207.0 eV), whereas, the Nb $3d_{5/2}$ bands of Pd-Nb and Pd-Nb-C were shifted to higher values, around 207.8 eV. In spite of these differences in binding energies, all the bands can be assigned to Nb(V) in Nb_2O_5[33], although it seems clear that an interaction with ceria exists that modifies the electronic properties of niobia. On the other hand, a small difference in binding energy is also detected in the ceria-free catalysts. Thus, the Nb $3d_{5/2}$ band in Pd-Nb-C appears at a somewhat higher binding energy than in Pd-Nb, where the support is bulk Nb_2O_5. This difference can be attributed to the higher dispersion of niobia on the support[34].

The XPS Ce/Nb atomic ratios of the two Ce-containing catalysts were 0.74 for Pd-Nb-Ce and 1.22 for Pd-Nb-Ce-C. Thus, there was a higher surface enrichment with ceria in the carbon-supported catalyst which is in good agreement the higher levels of reduced ceria observed for this catalyst. It should be noted that the bulk Ce/Nb ratio for these catalysts is 0.11.

The Pd 3d level X-ray photoelectron spectra for the reduced catalysts are compared in Fig. 7. The experimental spectra show

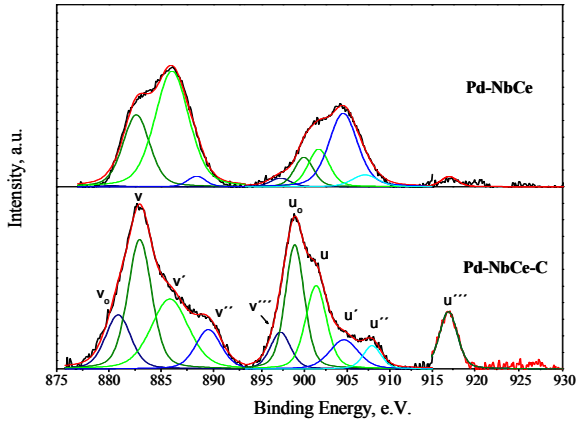

Fig 5. XPS Ce 3d spectra for the Ce-containing catalysts reduced at 528 K.

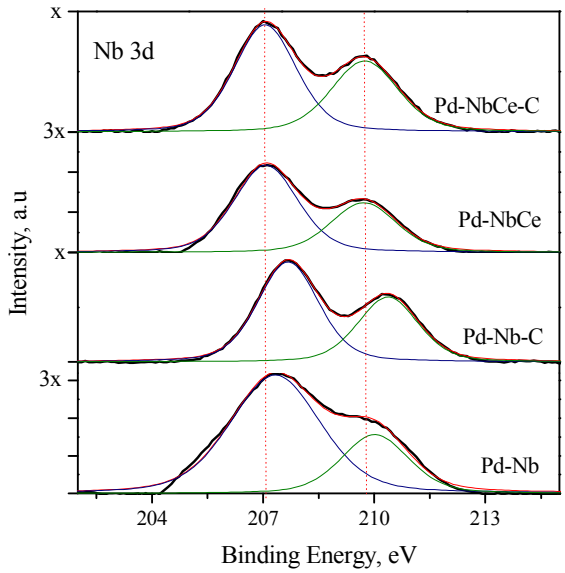

Fig. 6. XPS Nb 3d spectra for the catalysts, reduced at 528 K.

two bands corresponding to the Pd $3d_{5/2}$ (at higher binding energy) and Pd $3d_{3/2}$ (at lower binding energy) levels. For the former, a symmetric band centred at 337.3 eV is obtained for palladium supported on pure niobia and Ce-doped niobia. These bands were broader for the carbon-supported catalysts, thereby allowing deconvolution into two contributions. The Pd $3d_{5/2}$ binding energy of metallic palladium is reported to appear around 335.0 eV, whereas that for Pd^{2+} species ranges from 336.0 to 337.0 eV[35-39]. However, values as high as 335.7 eV have been also reported for metallic palladium in Pd/Al_2O_3[40]. With this in mind, bands in Fig. 7 should be in principle assigned to oxidized Pd species (Pd^{2+}). The larger broadness of the bands obtained with the carbon-supported catalysts can be explained by the presence of different Pd species arising from the complexity of these systems. However, binding energy values as high as 337.1-337.3 eV have been found for metallic Pd in Pd/Al_2O_3-CeO_2 catalysts, and they have been assigned to the interaction of small Pd clusters with the support[40-42]. The presence of metallic palladium in the catalysts is necessary to hydrogenate pentenoic acid, the intermediate in the formation of PA. Thus, from the XPS results it can be concluded that Pd is in the form of small metallic clusters with a high interaction with the oxide supports/promoters. Dispersion of oxides on the activated carbon support favors this interaction, maybe be due to the smaller particle size of the oxide crystallites, thereby resulting in a more heterogeneous distribution of Pd species. As will be discussed in the next section, this interaction appears to have interesting effects on the behavior of these catalysts in the title reaction.

3.2 Catalytic Activity

In a recent paper[43], Serrano-Ruiz et al. compared the behaviour of a series of Pd/Nb_2O_5 catalysts in the transformation of GVL to PA under different reaction conditions (Pd loading, reaction temperature, partial hydrogen pressure and WHSV), and they found that these parameters strongly influenced the catalytic behaviour. Their best result, in terms of selectivity to pentanoic acid, was obtained with a 0.1 wt.% Pd/Nb_2O_5 catalysts operating at 598 K, with a feed containing 50 wt.% GVL in water and hydrogen diluted in helium (50:50). Under these conditions, they obtained 92% selectivity to pentanoic acid, with small amounts of carbon oxides (CO_x, 1%) and C_4-C_5 alkanes (5%) accounting for the rest of products.

Fig. 8 shows the catalytic performance of the different catalysts studied in this work in terms of GVL conversion and selectivity to PA. After reaction, analyses of both the gas phase and of the liquid phases, aqueous and organic, were carried out.

Reaction products were detected neither in the gas phase nor in the liquid aqueous phase at the reaction conditions used in the present study. PA was thus the main product detected in the organic liquid phase, with only small amounts of 5-nonanol as by-product. Thus, selectivity to the desired product, PA, was very high (around 90 %) for all the catalysts, as shown in Fig. 8. The main difference among the catalysts was their activity. The values represented in Fig. 8 (average conversion from 24 to 30 h on-stream) ranged from 18% for Pd-NbCe to around 60% for Pd-Nb and Pd-Nb-C and, interestingly, 90% for Pd-NbCe-C. Thus, the Ce-free catalysts behave similarly irrespective of the use of the activated carbon support, but the dispersion of the active phases does have an important effect in the Ce-containing catalysts.

As indicated above, the first step in the catalytic transformation of GVL into PA is the ring opening to yield pentenoic acid, which is catalyzed by acid sites at the niobia surface. Then, pentenoic acid is hydrogenated to PA on the Pd metallic sites. As both Pd-Nb and Pd-Nb-C catalysts show similar behaviour in terms of both conversion and selectivity, it can be concluded that the dispersion of the active phases on the carbon support hardly modifies the activity of the catalyst, in spite of the fact that the number of acid sites strongly increased upon supporting on carbon (see NH_3-TPD results in Fig. 4). This behaviour suggests that the strength of the acid sites in the cerium-free catalysts is sufficient to achieve quasi-equilibrated ring-opening of GVL regardless their number, and the overall catalytic activity is thus controlled by the number of Pd surface sites that carry out the hydrogenation step. In the case of cerium-containing catalysts, strong differences in conversion were

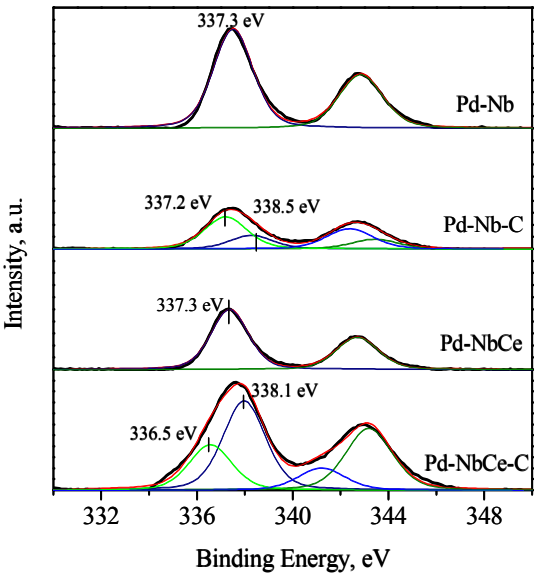

Fig. 7. XPS Pd 3d spectra for the catalysts, reduced at 528 K.

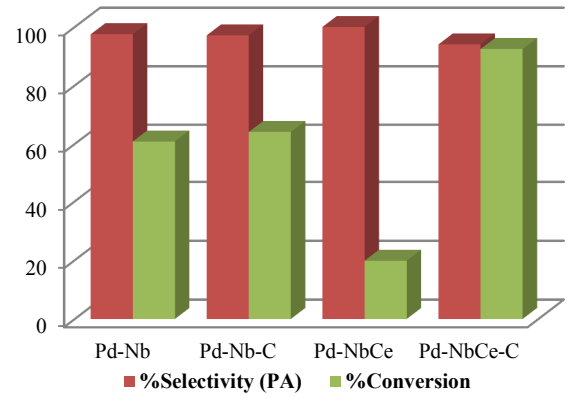

Fig. 8. Catalytic results in terms of conversion and selectivity to pentanoic acid (PA). 598 K, 0.05 mL·min^{-1} (GVL 60%), 34 Bar, 0.5 g of catalyst, He/H_2 flow 80/20 mL·min^{-1}.

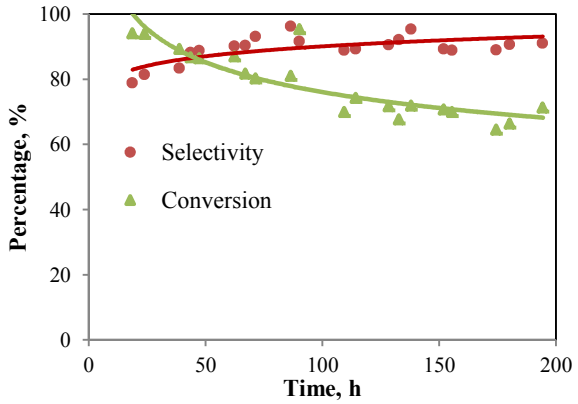

Fig. 9. GVL conversion and selectivity to PA for the Pd-NbCe-C during 200h reaction test. Reaction conditions are similar to those indicated in Fig. 8.

observed. Thus, while the unsupported Pd-NbCe catalyst showed a poor conversion (a third of that of Pd-Nb), the carbon-supported Pd-NbCe-C catalyst achieved nearly 90% conversion without loss of selectivity towards PA (Fig. 8). The strong decrease in activity observed for Pd-NbCe can be attributed to the drastic decrease in the strength of acid sites upon ceria addition (Fig. 4). In this case, the strength of acid sites would not be sufficiently high to achieve effective ring-opening of GVL, and the overall catalytic activity would be thus limited by the concentration of acid sites.

Since, as indicated by the NH_3-TPD analysis, both Pd-NbCe-C and Pt-Nb-C show similar surface acidity characteristics, the strong enhancement in activity found the cerium-containing catalysts has to be explained in terms of a beneficial effect of ceria over the Pd metallic phase (e.g., improving Pd dispersion and/or by modifying the electronic properties of Pd).In this way, XPS analysis revealed a high degree of ceria reduction in Pd-NbCe-C. Partial reduction of ceria leads to CeO_x non-stoichiometric phases with n-type semiconductor properties, thereby favouring electron density transfer to Pd particles in close contact with reduced ceria. In fact, XPS analysis of the Pd $3d_{5/2}$ level (Fig. 7) showed a band broadening with a contribution at C=C double bond in the adsorbed pentenoic acid, this facilitating its subsequent hydrogenation to PA. A similar effect has been observed in the hydrogenation of 1,3-butadiene on Pd/CeO_2, which has been shown to be promoted by sites at the Pd-Ce interface[44]. The authors concluded that the Pd-Ce interaction, induced after the reduction treatment, affected the adsorption strength of the 1,3-butadiene molecule. It should be noted that the reduction temperature used in this study, 538 K, is too low as to induce a strong Pd-ceria interaction that could lead to catalyst deactivation.

In order to assess the practical applicability of these catalysts, the one with the best performance (Pt-NbCe-C) was subjected to a long time reaction test (200 h) at the same reaction conditions than employed before, and results are exposed in Fig. 9. It can be seen that the catalyst slightly deactivated during the first 100 h on stream, with a loss of conversion of about 30%, but then it stabilized up to at least 200 h on stream. On the other hand, selectivity to pentanoic acid remains high (90% and stable during the 200 h period). These results contrast with the strong deactivation obtained with Pd supported on commercial niobia materials[40] and are indicative that the Pd-NbCe-C system is a very promising catalyst to be used in the transformation of GVL into PA.

4. Conclusions

This study shows the excellent performance of a carbon-supported Pd-NbCe catalyst in the production of PA via GVL ring opening and hydrogenation. The ring opening reaction takes place at the acid sites of niobia, whereas the hydrogenation of pentenoic acid to pentanoic acid occurs on the metal Pd particles. The importance of dispersing the active phases over the carbon support has been clearly evidenced. Thus, the surface acidity of the catalysts is enhanced and the interaction between the noble metal and cerium oxide is favoured, which in turn facilitates the hydrogenation of pentenoic acid by improving the catalytic properties of Pd. Studies at long reaction times showed that this material is a promising catalyst for this interesting reaction, an

important step in the synthesis of green hydrocarbons.

Acknowledgements

Financial support from Ministerio de Ciencia e Innovación (Spain) (MAT2010-21147) is gratefully acknowledged. R.B. thanks UA, CAM and Unión Fenosa for his predoctoral grant (UF2007-X9159987F).

Notes and references

[a] *Laboratorio de Materiales Avanzados. Departamento de Química Inorgánica - Instituto Universitario de Materiales de Alicante, Universidad de Alicante. Apartado 99, E-03080 Alicante, Spain. E-mail: asepul@ua.es; Fax: +34 965903454; Tel: +34 965903974*

[b] *Department of Chemical and Biological Engineering, University of Wisconsin-Madison, Wisconsin 53706, USA.*

Reference List

1 D. Tilman, R. Socolow, J. A. Foley, J. Hill, E. Larson, L. Lynd, S. Pacala, J. Reilly, T. Searchinger, C. Somerville and R. Williams, *Science*, 2009, **325**, 270.

2 G. W. Huber and A. Corma, *Angew. Chem. Int. Ed.*, 2007, **46**, 7184.

3 W. H. George and E. D. Bruce, *Scient. Amer.*, 2009, **301**, 52.

4 D. M. Alonso, J. Q. Bond and J. A. Dumesic, *Green Chem.*, 2010, **12**, 1493.

5 J. C. Serrano-Ruiz, D. J. Braden, R. M. West and J. A. Dumesic, *Appl. Catal. B: Environ.*, 2010, **100**, 184.

6 D. M. Alonso, J. Q. Bond, J. C. Serrano-Ruiz and J. A. Dumesic, *Green Chem.*, 2010, **12**, 992.

7 I. E. Wachs, J. M. Jehng, G. Deo, H. Hu and N. Arora, *Catal. Today*, 1996, **28**, 199.

8 T. Ushikubo, *Catal. Today*, 2000, **57**, 331.

9 E. Ramos-Fernández, J. Serrano-Ruiz, J. Silvestre-Albero, A. Sepúlveda-Escribano and F. Rodríguez-Reinoso, *J. Mater. Sci.*, 2008, **43**, 1525.

10 J. C. Serrano-Ruiz, A. Sepúlveda-Escribano, F. Rodríguez-Reinoso and D. Duprez, *J. Mol. Catal. A: Chem.*, 2007, **268**, 227.

11 J. C. Serrano-Ruiz, A. Sepúlveda-Escribano and F. Rodríguez-Reinoso, *J. Catal.*, 2007, **246**, 158.

12 J. C. Serrano-Ruiz, E. V. Ramos-Fernández, J. Silvestre-Albero, A. Sepúlveda-Escribano and F. Rodríguez-Reinoso, *Mater. Res. Bull.*, 2008, **43**, 1850.

13 J. C. Védrine, G. Coudurier, A. Ouqour, P. G. Pries de Oliveira and J. C. Volta, *Catal. Today*, 1996, **28**, 3.

14 T. Ohuchi, T. Miyatake, Y. Hitomi and T. Tanaka, *Catal. Today*, 2007, **120**, 233.

15 L. Li and Y. Chen, *Mater. Sci. Engineer.: A*, 2005, **406**, 180.

16 I. Nowak, M. Misiewicz, M. Ziolek, A. Kubacka, V. Cortés Corberán and B. Sulikowski, *Appl. Catal. A: Gen.*, 2007, **325**, 328.

17 J. M. Jehng and I. E. Wachs, *Chem. Mater.*, 1991, **3**, 100.

18 B. X. Huang, K. Wang, J. S. Church and Y. S. Li, *Electrochim. Acta*, 1999, **44**, 2571.

19 S. Kunjara Na Ayudhya, A. Soottitantawat, P. Praserthdam and C. Satayaprasert, *Mater. Chem. Phys.*, 2008, **110**, 387.

20 J. R. McBride, K. C Hass, B. D.Poindexter and W. H. Weber, *J. Appl. Phys.*, 1994, **76**, 2435.

21 I. Kosacki, T. Suzuki, H. U. Anderson and P. Colomban, *Solid State Ionics*, 2002, **149**, 99.

22 C. L. T. da Silva, V. L. L.Camorim, J. L. Zotin, M. L. R. Duarte Pereira and A. D. C. Faro Jr., *Catal. Today*, 2000, **57**, 209.

23 M. Paulis, M. Martín, D. B. Soria, A. Díaz, J. A. Odriozola and M. Montes, *Appl. Catal. A: Gen.*, 1999, **180**, 411.

24 P. Burroughs, A. Hamnett, A. F. Orchard and G. Thornton, *J. Chem. Soc., Dalton Trans.*, 1976, 1686.

25 A. Laachir, V. Perrichon, A. Badri, J. Lamotte, E. Catherine, J. C. Lavalley, J. El Fallah, L. Hilaire, F. Le Normand, E. Quemere, G. N. Sauvion and O. Touret, *J. Chem. Soc., Faraday Trans.*, 1991, **87**, 1601.

26 M. S. Francisco, V. R. Mastelaro, P. A. P. Nascente and A. O. Florentino, *J. Phys. Chem. B*, 2001, **105**, 10515.

27 B. Ernst, L. Hilaire and A. Kiennemann, *Catal. Today*, 1999, **50**, 413.

28 J. Silvestre-Albero, F. Rodríguez-Reinoso and A. Sepúlveda-Escribano, *J. Catal.*, 2002, **210**, 127.

29 P. W. Park and J. S. Ledford, *Langmuir*, 1996, **12**, 1794.

30 I. K. Naik and T. Y. Tien, *J. Electrochem. Soc*, 1979, **126**, 562.

31 N. Özer, D. G. Chen and C. M. Lampert, *Thin Solid Films*, 1996, **277**, 162.

32 Roland Benoit CNRS Orléans, in: www.lasurface.com, 2012).

33 V.V. Alegre, M.A.P.da Silva and M.Schmal, *Catalysis Communications*, 2006, **7**, 314.

34 S. Damyanova, L.Dimitrov, L.Petrov and P.Grange, *Applied Surface Science*, 2003, **214**, 68.

35 G.B. Hoflund, H.A.E.Hagelin, J.F.Weaver and G.N.Salaita, *Applied Surface Science*, 2003, **205**, 102.

36 W. Huang, Z.Zuo, P.Han, Z.Li and T.Zhao, *Journal of Electron Spectroscopy and Related Phenomena*, 2009, **173**, 88.

37 H. Karhu, A.Kalantar, I.J.Väyrynen, T.Salmi and D.Y.Murzin, *Applied Catalysis A: General*, 2003, **247**, 283.

38 Y. Deng, T.G.Nevell, R.J.Ewen and C.L.Honeybourne, *Applied Catalysis A: General*, 1993, **101**, 51.

39 A. Gniewek, A.M.Trzeciak, J.J.Ziólkowski, L.Kepinski, J.Wrzyszcz and W.ylus, *Journal of Catalysis*, 2005, **229**, 332.

40 H. Pham, Y. Pagan-Torres, J.C. Serrano-Ruiz, D. Wang, J. A. Dumesic, D. K. Abhaya. *Applied Catalysis A: General*, 2011, **397,** 153.

41 J. Libra and V. Matolín, *Surf. Sci.,* 2006, **600,** 2317.

42 N. Tsud, V. Johánek, I. Stará, K. Veltruská and V. Matolín, *Surf. Sci.,* 2000, **467,** 169.

43 J.C. Serrano-Ruiz, D. Wang and J.A. Dumesic, *Green. Chem.,* 2010, **12,** 574.

44 R. Monteiro, F.B. Noronha, L.C. Dieguez and M. Schmal, *Appl. Catal. A: Gen.,* 1995, **131,** 89.